Electronic Supplementary Information

An experimental and computational framework for engineering multifunctional nanoparticles: designing selective anticancer therapies.

Antonio Aires, Jael F. Cadenas, Raúl Guantes,* and Aitziber L. Cortajarena*

NP characterization

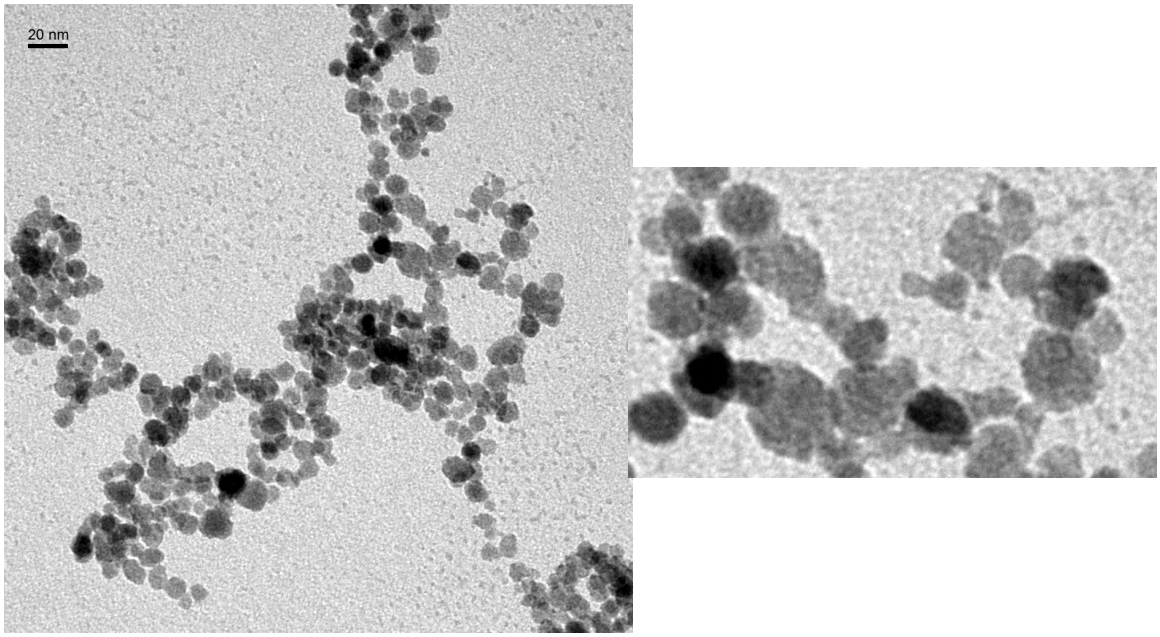

Figure S1. TEM micrographs of BSA-NPs. On the right, zoom in image in which the lighter layer of protein coating around the core can be slightly observed.

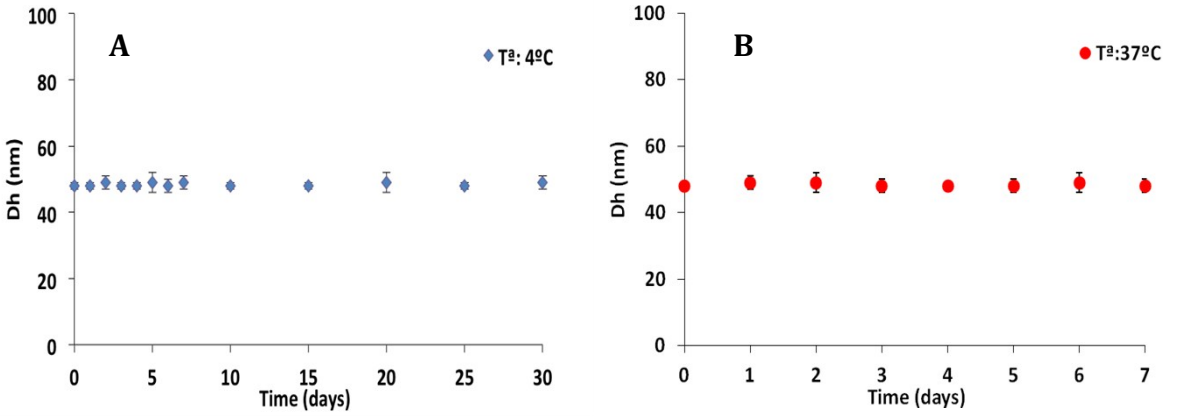

Figure S2. Stability of BSA-NPs. Variation of the hydrodynamic diameter (nm) of BSA-NPs monitored by DLS over time at 4ºC (A) and 37ºC (B). The data show that the nanoformulation is stable at least 1 month at 4ºC and at least one week at 37ºC.

Drug release studies

In order to evaluate the stimuli-response of the BSA-NP-GEM and BSA-MNP-GEM-N6L under reducing environment, the GEM drug release was monitored at 37°C in 0.01 M sodium phosphate, pH 7.4 using 1μM or 1 mM of DTT to mimic the extracellular and intracellular conditions, respectively (Figure S3).

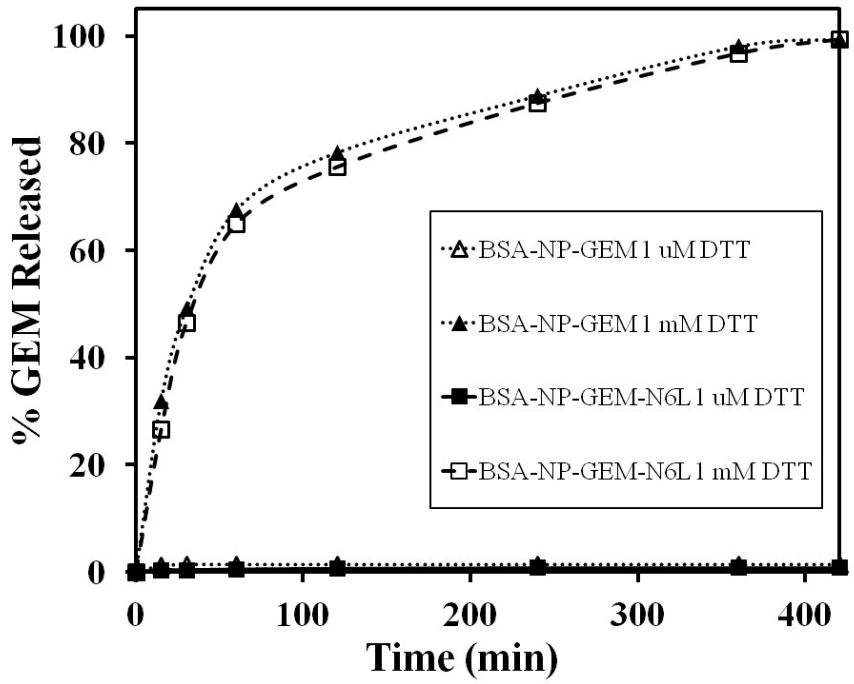

Figure S3. Release kinetics of GEM from BSA-NP-GEM and BSA-NP-GEM-N6L under weak and strong reducing conditions mimicking the extracellular and intracellular environment, respectively.

Internalization of NPs in MCF-10A cells

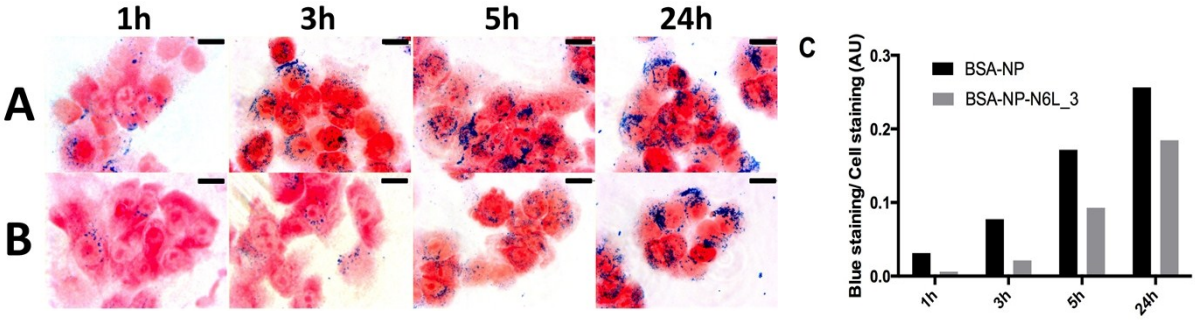

Figure S4. Prussian blue staining of MCF-10A cells incubated with BSA-NP (A) and BSA-NP-N6L_3 (B) for 1, 3, 5 and 24 h at 37°C (scale bar = 10 μm). C. NP blue staining density values relative to phenol red cell density values expressed in arbitrary units (AU) after 1, 3, 5 and 24 h of treatment with BSA-NP (black bars) BSA-NP-N6L_3 (grey bars).

Intracellular localization of NPs by confocal reflection microscopy

To verify the specific targeting of breast cancer cells (MDA-MB-231) in comparison with non-tumorigenic cells (MCF-10A) with BSA-NP-N6L_3 in the selected conditions, we performed confocal reflection microscopy studies that allow the visualization of the nanoparticle core at the different confocal planes (Figure S5).

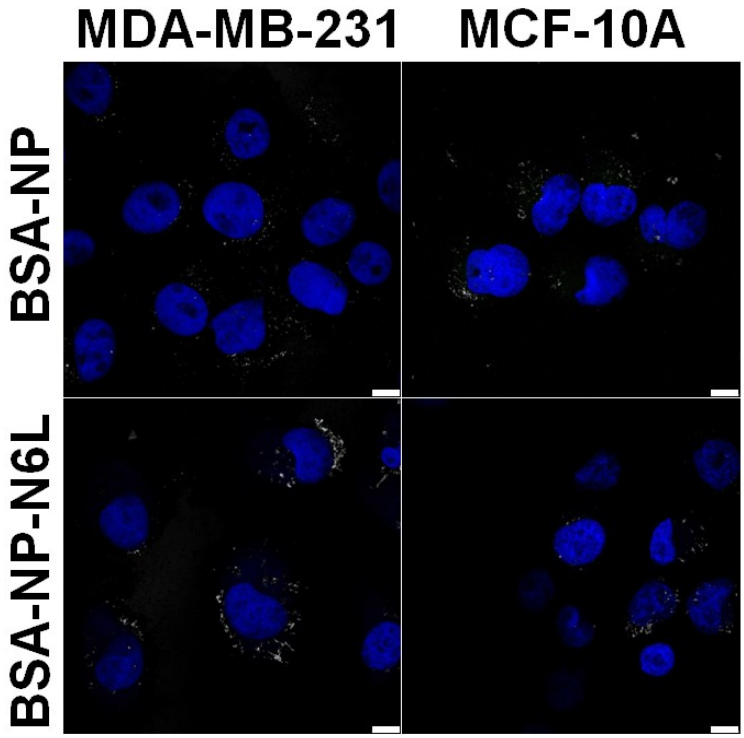

Figure S5. Cellular localization of BSA-NP and BSA-NP-N6L_3 in MDA-MB-231 and MCF-10A. Cells were incubated for 5 h with 0.2 mg Fe mL^{-1} of BSA-NP and BSA-NP-N6L_3. Cells were fixed and stained right after NP incubation. Cells were observed using confocal fluorescence in combination with reflection microscopy, detecting signals from the nucleus by DAPI nucleic acid stain (blue), and reflected light from NPs (white spots) (scale bar = 10 μm).

Model description

The model developed includes the following assumptions:

- No diffusion or spatial effects are considered. Nanoparticles (NP) are supposed to be homogeneously distributed in the culture media, with an average number of available NP per cell. Similarly, receptors are assumed to be homogeneously distributed on the cell's surface, with R_T representing the average number of

specific receptors per cell. For our system, the experimental range of concentrations gives (see below) an average number of NP per cell between $7x10^7$ and $2.8x10^8$. With such high numbers of NP per cell, we can safely assume that inhomogeneities play a minor role. Moreover, microscopy images of our cell culture show that cells are not very confluent, so that NP can reach all cells in the culture medium.

- The conservation equation for R_T, Eq. (5) in the main text, holds only if there is complete receptor recycling after internalization of each NP/receptor complex C_i. Similarly, effects of receptor trafficking inside the cytoplasm, or receptor production/degradation[1] are not considered. Incomplete receptor recycling can be taken into account within our model by defining a new equation for the number of free receptors on the surface:

$$\frac{dR}{dt} = -nk_{on}NP_f R + k_{off}C_1 - k_c R\sum_{i=1}^{n-1}(n-i)C_i + k_{-c}\sum_{i=2}^{n} iC_i + k_e f_R \sum_{i=1}^{n} i \cdot C_i$$

where $0 \le f_R \le 1$ is the recycling fraction for receptors. Effects of receptor recycling are important only if NP uptake is measured at times comparable to the saturation time for internalization, which is not our case (after 24h, our formulation has not yet reached saturation).[2]

- We did not consider exocytosis of NP once they are internalized, although for small NP it can be noticeable. The measured hydrodynamic diameter of our iron NP is between 50 and 80 nm. For gold NP in HeLa cells, the fraction of particles exocytosed at 5h was around 20% for 50 nm NPs, and ~7% for 74 nm NP[3].
- The non-specific uptake dependence on N6L dose is the same for both cell lines. This is not justified in principle, since extracellular medium and membrane properties can differ in normal and cancer cells. However, this simplifies our analysis and allows testing our hypothesis that increased NP uptake with N6L

dose in cancer cells is due to specific binding to N6L receptors.

- The endocytosis rate constant, k_e, is assumed to be the same for all NP bound to membrane by specific receptors, independently of the number of N6L ligands involved. This assumption is made for simplicity, but we acknowledge that this may not be the case, since deformation and wrapping of the cell membrane to form endosomes depends on the density of ligands on the particle surface, as well as on particle size[4, 5]. We think however that with the size of the NP (~50 nm) and number of ligands experimentally attached (a maximum of 8 ligands per NP) this effect should be small. Another possible effect is that the number of ligand-receptor bonds influences recruitment of adaptor proteins or actin necessary for clathrin mediated endocytosis[6, 7].
- The crosslinking association and dissociation constants, k_c and k_{-c} respectively, are assumed to be the same for all complexes C_i (a usual assumption in this type of models).

Calibration of the non-specific uptake rate

The phenomenological non-specific uptake rate, $\alpha_{ns}(N6L)$, is fitted to the observed dependence of internalized NP after 5h of incubation in healthy cells, since specific uptake in this cell line is assumed to be low. The N6L dependence of internalization is well described by an inverse Michaelis-Menten function of the form (see Figure 3):

$$\alpha_{ns}(N6L) = \frac{\alpha_0}{1 + N6L/K_m} \quad (S1)$$

with a Michaelis constant K_m=1.27. The non-specific uptake rate for NP without N6L pseudopeptide, α_0, can be obtained by noting that in this case, the number of NP internalized, NP_i, changes according to the equation:

$$\frac{dNP_i}{dt} = \alpha_0 \cdot NP_f = \alpha_0\left(NP_f^0 - NP_i\right) \qquad (S2)$$

where NP_f^0 is the initial number of free NP per cell effective medium, and in the last equality we assumed NP conservation, $NP_f^0 = NP_f + NP_i$. The solution of this simple equation is

$$NP_i(t) = NP_f^0\left(1 - e^{-\alpha_0 \cdot t}\right), \qquad (S3)$$

and solving for α_0 we get:

$$\alpha_0 = \frac{1}{t_{inc}} \cdot ln\left(\frac{NP_f^0}{NP_f^0 - NP_i^{ex}}\right) \quad (S4)$$

where t_{inc} is the incubation time of cells with NP (5h) and NP_i^{ex} is the experimentally measured number of non-functionalized NP internalized after this time.

The simplification that the non-specific uptake rate for non-targeted NP, α_0, is constant, implies from equation (S3) that, for a fixed incubation time, the amount of particles internalized is proportional to the concentration of NP in solution. To check whether this simplification captures a real experimental situation, we treat MDA-MB-231 cells with different NP formulations: functionalized NP alone, and functionalized NP coated with 4 molecules of N6L per NP, at concentrations of 0.05, 0.075, 0.1, 0.15 and 0.2 mg Fe/ml for both formulations. We calibrated the value of α_0 from (S4) using the experimental number of internalized NP at the highest concentration, 0.2 mg Fe/ml (we assume that at large NP concentrations the effect of diffusion or inhomogeneities in the cell milieu is minimal). We then calculate the number of internalized NP after 5 hours at different concentrations, using equation (S3) for the NP alone formulation, and equations (1)-(4) in the main text (multivalent ligand model) with *n=4* for the NP+N6L formulation. The theoretical results for both formulations are shown with solid lines in

Figure S6, while experimentally obtained internalization values are shown with circles.

We see that, despite this simplification, the experimental trend of NP internalization at different concentrations is quantitatively reproduced for both treatments (NP alone and NP+4N6L) without further model adjustment. We notice that the rest of the parameters used for the multivalent-ligand model, equations (1)-(4), are taken from the fitting to the internalization versus N6L dose curve, Figure 3 (see below). Thus, the parameters obtained fitting experimental results at the largest concentration of NP can be consistently used to reproduce different concentrations and formulations.

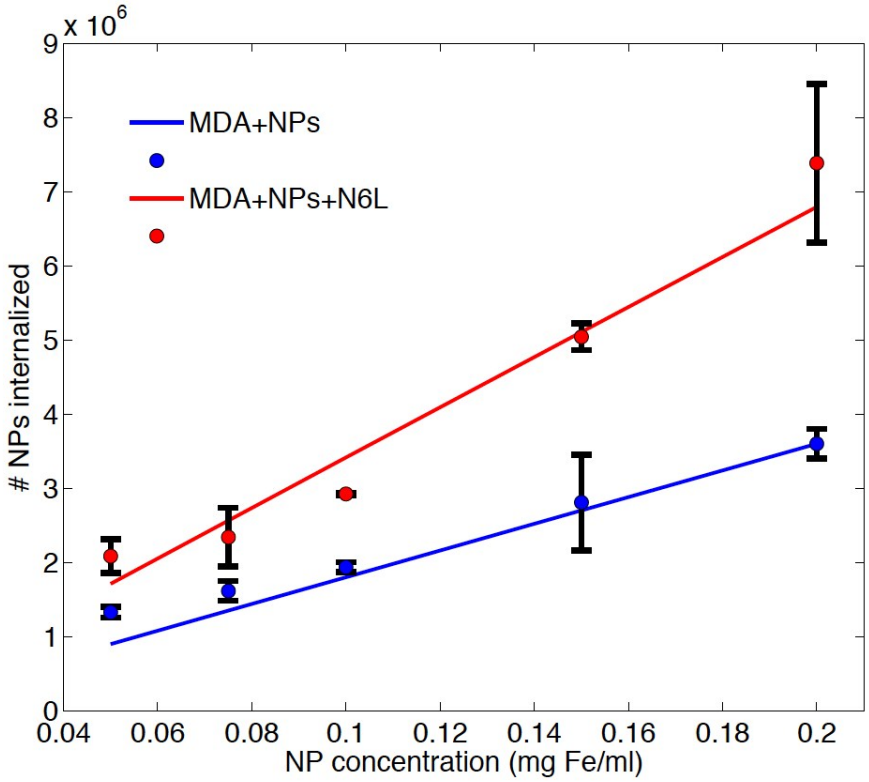

Figure S6. Number of NP internalized by MDA-MB-231 cells using a formulation of functionalized NP alone (BSA-NP) (blue line and symbols) and NP coated with 4 N6L molecules (BSA-NP-N6L_3) (red line and symbols), at different initial concentration of NP (0.05, 0.075, 0.1, 0.15 and 0.2 mg Fe/ml). Lines are model results (equations (1)-(6) in main text), and circles are experimental values. Error bars are SD of three independent experiments.

Estimation of parameters and receptor fold-change abundances

In the case that NP are functionalized with only one molecule of N6L (monovalent ligand), the model equations are reduced to:

$$\frac{d\,NP_f}{dt} = -k_{on}NP_f R + k_{off}C_1 - \alpha_{ns}\cdot NP_f \quad (S5)$$

$$\frac{d\,C_1}{dt} = k_{on}NP_f R - (k_{off}+k_e)C_1 \quad (S6)$$

$$\frac{dR}{dt} = (k_{off}+k_e)C_1 - k_{on}NP_f R \quad (S7)$$

$$\frac{dNP_i}{dt} = k_e C_1 + \alpha_{ns}\cdot NP_f \quad (S8)$$

where C_1 is the complex formed by the specific receptor and the NP with one ligand molecule. Note that we do not calculate the number of internalized NP (NP_i) from the conservation constraint $NP_f + NP_i + C_1 = NP_f^0$ as in the main text, but give an explicit equation for the dynamics of NP_i, equation (S8). Using the conservation constraint for the total number of receptors per cell, $R + C_1 = R_T$ together with the assumption that free ligand is in excess, $NP_f \approx NP_f^0$, equations (S5)-(S8) reduce to:

$$\frac{dR}{dt} = (k_{off}+k_e)R_T - (k_{off}+k_e + k_{on}NP_f^0)R \quad (S9)$$

$$\frac{dNP_i}{dt} = k_e R_T + \alpha_{ns}\cdot NP_f^0 - k_e R \quad (S10)$$

We note that at the concentration of NP used for the internalization experimental data in Figure 3, $NP_f^0 \cong 3\cdot 10^8$ and the excess ligand approximation should be valid. We checked this assumption numerically solving equations (S5)-(S8) and comparing against the results of eqs. (S9)-(S10), showing that this approximation is extremely accurate for the concentrations and incubation times used in experiments.

The solution of eqs. (S9)-(S10) is:

$$R(t) = \frac{\alpha}{\beta}\left(1 - e^{-\beta t}\right) + R_T e^{-\beta t} \quad (S11)$$

$$NP_i(t) = \left(\gamma - k_e\frac{\alpha}{\beta}\right)t - k_e\mu e^{-\beta t} + k_e\mu \quad (S12)$$

where $\alpha \equiv (k_{off} + k_e)R_T$, $\beta \equiv k_{off} + k_e + k_{on}NP_f^0$, $\gamma \equiv \alpha_{ns}NP_f^0 + k_e R_T$ and $\mu \equiv \frac{1}{\beta}\left(\frac{\alpha}{\beta} - R_T\right)$.

For $t \equiv t_{inc} = 5h$ (incubation time) we know from the experiments at N6L=1 the number of particles internalized per cell, NP_i^{exp}, in both cell lines. Using this in eq. (S12) we can write:

$$NP_i^{exp} \cong \left(\gamma - k_e\frac{\alpha}{\beta}\right)t_{inc} + k_e\mu$$

We can rearrange this expression in the form:

$$c = \tau\left(\frac{1}{\beta} - \frac{1}{t_{inc}\beta^2}\right) \quad (S13)$$

where $c \equiv \frac{NP_i^{exp}}{t_{inc}} - \alpha_{ns}NP_f^0$ and $\tau \equiv k_e\, k_{on}NP_f^0R_T$. The left-hand side of equation (S13), the constant c, depends only on the experimentally measured value of internalized NP, NP_i^{exp}, and on the non-specific uptake rate α_{ns} which was estimated in the previous Section. These two quantities are different for healthy and tumor cells. The right-hand side of equation (S13) depends on the kinetic rates k_e, k_{off} and k_{on} (or K_D), which are assumed to be the same for both cell types, and the total number of receptors through the parameter τ. Equation (S13) allows us to estimate the fold-change in receptor concentration in both cell lines, knowing the internalized NP with N6L=1, as

$$\frac{R_T^t}{R_T^h} = \frac{\tau^t}{\tau^h} = \frac{c^t}{c^h} = \frac{\frac{NP_i^t}{t_{inc}} - \alpha_{ns}^t NP_f^0}{\frac{NP_i^h}{t_{inc}} - \alpha_{ns}^h NP_f^0} \quad (S14)$$

where the superindices t and h stand for tumor and healthy cells respectively. Using the experimentally measured values of $NP_i^{t,h}$ and $\alpha_{ns}^{t,h}$ we find that

$$\frac{R_T^t}{R_T^h} = 12.3 \quad (S15)$$

i.e., around a 10 fold-change in receptor abundance is consistent with the experimental internalization data of monovalent NP. When fitting parameters for the whole N6L dose experimental regime, we find that a fold-change of 20 is also consistent (within measurement errors) with the monovalent data, while producing a better adjustment of the overall internalization data. The rest of the kinetic parameters (k_e, k_{off}, K_D and K_C) determine the internalization of NP with larger doses of N6L, using eqs. (1)-(6) in the main text. To estimate these parameters, we first restricted the possible values of k_e and k_{off}. Notice that for a fixed value of K_D, equation (S13) implies that the total receptor number R_T is completely determined by k_e , k_{off} and the already known values of NP_i^{exp} and α_{ns}. This is shown as a contour plot in Figure S7.

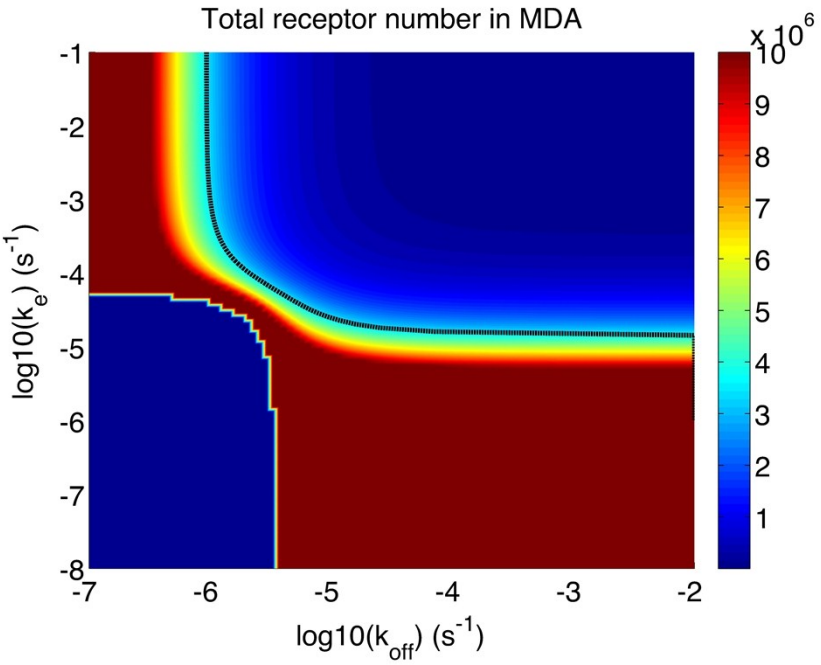

Figure S7. Color contour plot of total receptor number R_T in tumor cells as a function of the endocytic and unbinding constants k_e and k_{off}. We used K_D=3 nM. Black dashed line is the contour corresponding to R_T=3.5x10^6.

Meaningful receptor numbers are achieved for $k_e \sim 5 \cdot 10^{-6} - 0.1\ s^{-1}$, and $k_{off} \sim 5 \cdot 10^{-7} - 10^{-2}\ s^{-1}$. Then, we changed simultaneously receptor number of tumor cells between 10^6 and 5x10^6 [8] and varied k_e (with k_{off} determined by eq. (S13)) to find

the best fit to the experimental internalization data shown in Figure 3. We find that a set of parameters consistent with all internalization data shown both in Figure 3 and Figure S7 is K_D=3 nM, k_{off}=10^{-6} s^{-1}, k_e=10^{-2} s^{-1} and R_T=3.5x10^6 for tumor cells.

Notice that these parameters are the same for healthy cells, except the total receptor number, which is set by eq. (S14).

The number of NP internalized at different N6L doses obtained from these parameters in model simulations are shown with solid lines in Figure 3 of main text.

The parameters and units used throughout the text are summarized in Table S1.

Table S1. Model Parameters and Constants: Definitions and estimated/fitted values

Parameter	Meaning	Value	Reference
NP_f^0	Average number of free NP per cell surrounding medium	7x10^7-2.8x10^8	Estimated from the experimental concentrations 0.05-0.2 mgFe/ml*
k_{on}	N6L ligand/receptor association constant	1.2x10^{-3} $nM^{-1}h^{-1}$**	Calculated as $k_{on} = \frac{k_{off}}{K_D}$
k_{off}	N6L ligand/receptor dissociation constant	10^{-6} s^{-1}	Fitted to experimental data
K_D	Dissociation equilibrium constant for ligand/receptor binding	3 nM	Fitted to our experimental data in the range 0.5-10 nM [9, 10]
k_c	Crosslinking ligand/receptor association constant	3.6x10^{-3} $nM^{-1}h^{-1}$***	Calculated as $k_c = \frac{k_{-c}}{K_x}$
k_{-c}	Crosslinking ligand/receptor dissociation constant	10^{-6} s^{-1}	Ligand/receptor unbinding is assumed to be independent of the number of bounded ligands.
K_x	Crosslinking equilibrium constant	1 nM	Similar to 3D equilibrium constant K_D. See #
k_e	Endocytosis constant	10^{-2} s^{-1}	Fitted to experimental data.
α_0	Non-specific uptake rate	10^{-3} h^{-1} t	Estimated from

	of non-targeted NP (N6L=0)	$3.2\text{x}10^{-3}$ h^{-1} [h]	internalization data of non-targeted NP, Eq. (S4).
K_m	Michaelis constant for non-specific uptake dependence on ligand dose, Eq. (S1).	1.27 per ligand molecule	Fitted to internalization data of healthy cells.
R_T	Average number of specific surface receptors per cell	$3.5\text{x}10^{6}$ [t]	Fitted to experimental data.
		$3.5\text{x}10^{6}/20$ [h]	Estimated from experimental data with monovalent NP, Eq. (S14).

[*] Calculated as $NP_f^0 = \left[\frac{mgFe}{ml}\right] \cdot V_{cult} \cdot NP_{mgFe}/\#cells$, where $\left[\frac{mgFe}{ml}\right]$ is the concentration of the formulation in mg of Fe per ml, V_{cult} the volume of cell culture per well (0.5 ml), $\#cells$ the average number of cells per well (50,000), and NP_{mgFe} the number of NP present in a mg of Fe ($1.4\text{x}10^{14}$ calculated from manufacturer specifications).

[**] In model simulations, free ligand is given as number of NP per cell surrounding medium. Therefore the association constant (in units of $nM^{-1}h^{-1}$) should be scaled as $k_{on} \cdot 10^9 \cdot V_{eff}/N_{Av}$, where V_{eff} is the effective volume of extracellular medium per cell (10^{-2} microliters) and N_{Av} is Avogadro's number.

[***] Since cross-linking reactions take place on the cell surface, and the variable C_i represents the number of cross-linked ligand/receptor complexes on the cell membrane, the cross-linking association constant is scaled as $k_c \cdot 10^9 \cdot V_{surf}/N_{Av}$ where V_{surf} is the effective volume for reactions on the cell surface. This is calculated as $V_{surf} = 4\pi r^2 h$, where r is the cell radius (15 μm) and h is the estimated membrane thickness (8 nm)[1].

[#] This assumes that cross-linking reactions are not facilitated by enhanced diffusion on the surface (or by smaller reaction volumes once the NP is already attached to the surface[1]). This is expected to approximately hold in our experimental situation where we have an excess of free NP in solution. We performed numerical simulations varying K_x in the range 10^{-1}-100 nM. The number of internalized NP were similar within the whole range of experimental N6L doses (until N6L=8) and only differ at large N6L doses (N6L>10), where we do not have experimental accessibility.

[t] Tumor cells.

[h] Healthy cells.

Effect of multivalency on binding affinity

By analogy with a simple process of ligand/receptor binding,

$$L + R \underset{k_{off}}{\overset{k_{on}}{\rightleftarrows}} C$$

where the dissociation constant is defined in terms of equilibrium values of the molecular species as

$$K_D = \frac{k_{off}}{k_{on}} = \frac{R^{eq} L^{eq}}{C^{eq}},$$

we can define an 'effective affinity' constant or avidity, K_A, for our multivalent process with n binding sites as

$$K_A = \frac{1}{K_D} = \frac{\sum_{i=1}^{n} C_i^{eq}}{R^{eq} NP_f^0} \quad (S16)$$

Here we have used the excess ligand approximation $NP_f^{eq} \cong NP_f^0$, and we recall that C_i stands for the number of NP bound to the cell by i binding sites. The multivalent binding equations (1)-(4) in the main text can be solved at equilibrium[11] which, together with the conservation relations (5) and (6), allows to calculate the avidity as:

$$K_A = \frac{\left(\frac{R^{eq}}{K_C} + 1\right)^n - 1}{K_D \cdot \frac{R^{eq}}{K_C}} \quad (S17)$$

where K_C is the crosslinking dissociation constant, $K_C = k_c / k_{-c}$.

The amount of free receptors per cell at equilibrium, R^{eq}, can be obtained by numerically solving the equation

$$\frac{R^{eq}}{R_T}\left\{1 + n\frac{NP_f^0}{K_D}\left(\frac{R^{eq}}{K_C} + 1\right)^{n-1}\right\} = 1 \quad (S18)$$

In the limit of negligible crosslinking ($k_{-c} \gg k_c$), i.e., when the NP behaves as an effective monovalent ligand, equation (S16) becomes

$$K_A = \frac{n}{K_D} \quad (S19)$$

To get an idea of how the binding affinity increases in our system due to the possibility of crosslinking reactions between the available ligand sites and the surface receptors, we show in Figure S8 the avidity in our two model systems as a function of the number of N6L ligand molecules per NP.

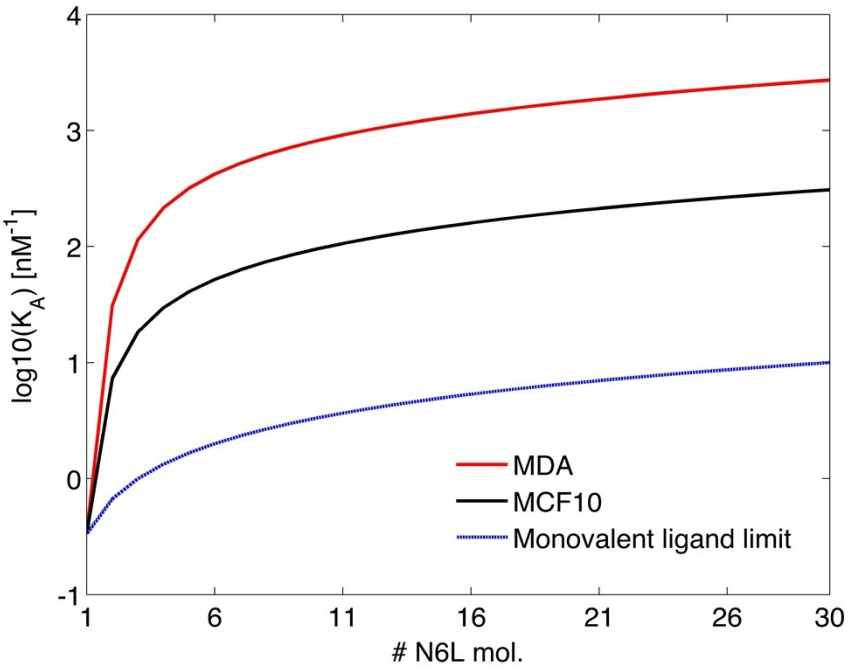

Figure S8. Avidity, calculated from eq. (S17) for the tumor cell line (MDA-MB-231) and for the healthy cell line (MCF-10A). The limit of monovalent ligand, eq. (S19), is shown in blue. Model parameters are given in Table S1.

We note that our reference value is the monovalent situation (NP functionalized with only one molecule of N6L), $K_A = K_D^{-1} = 0.33$ nM^{-1}. Functionalizing with many ligand molecules (N6L > 6) increases binding affinity in cancer cells by more than three orders of magnitude.

Correspondence between internalization and survival data in MDA-MB-231 cell line

To check the consistency between experimental internalization data, model simulations and cell survival, we combined the experimental internalization data at different concentrations shown in Figure S6 (with N6L=0 and N6L=4) with the experimental results for the survival fraction of cells after 6 days post-treatment using the same concentrations and N6L doses (coating NP with 22 molecules of gemcitabine). We show in Figure S9 the survival-internalization dependence using experimental data for both quantities (open symbols) and simulating internalization with the mathematical model (blue filled symbols). Despite these results are combined from different sets of experiments, they show there is monotonic correspondence between NP uptake and long-term survival, also consistent with model predictions.

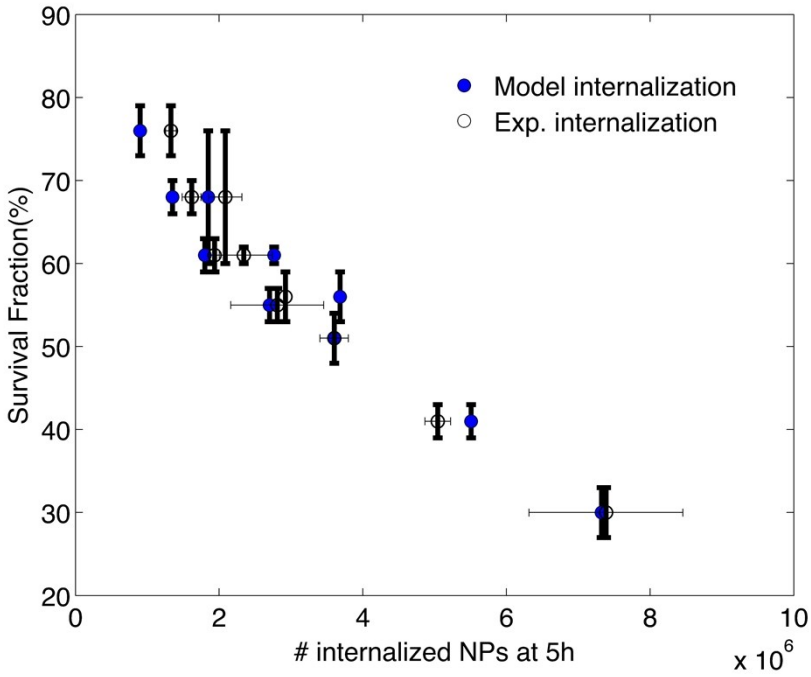

Figure S9. Internalization of NP in MDA-MB-231 cells, after 5h of incubation with two different formulations (non-functionalized NP and NP+4N6L) at the concentrations shown in Figure S6, versus survival fraction of cells after 6 days of treatment using the same formulations and concentrations. Open circles are experimental results (error bars are SD of three independent experiments), and filled circles correspond to internalization data simulated with the model.

References

1. D. A. Lauffenburger and J. J. Linderman, *Receptors: Models for binding, trafficking, and signaling*, Oxford University Press, New York, 1993.
2. M. C. Sader, P.; Carpentier, G.; Gilles, M.-E.; Bousserrhine, N.; Livet, A.; Cascone, I.; Destouches, D.; Cortajarena, A.L.; Courty, J., *Nanomedicine and Nanotechnology*, 2015, **6**, 1000299.
3. B. D. Chithrani and W. C. Chan, *Nano Lett*, 2007, **7**, 1542-1550.
4. H. Gao, W. Shi and L. B. Freund, *Proc Natl Acad Sci U S A*, 2005, **102**, 9469-9474.
5. S. Zhang, H. Gao and G. Bao, *ACS Nano*, 2015, **9**, 8655-8671.
6. I. Canton and G. Battaglia, *Chem Soc Rev*, 2012, **41**, 2718-2739.
7. M. Kaksonen, C. P. Toret and D. G. Drubin, *Nat Rev Mol Cell Biol*, 2006, **7**, 404-414.
8. S. Hauert, S. Berman, R. Nagpal and S. N. Bhatia, *Nano Today*, 2013, **8**, 566-576.
9. D. Destouches, E. Huet, M. Sader, S. Frechault, G. Carpentier, F. Ayoul, J. P. Briand, S. Menashi and J. Courty, *J Biol Chem*, 2012, **287**, 43685-43693.
10. D. Destouches, N. Page, Y. Hamma-Kourbali, V. Machi, O. Chaloin, S. Frechault, C. Birmpas, P. Katsoris, J. Beyrath, P. Albanese, M. Maurer, G. Carpentier, J. M. Strub, A. Van Dorsselaer, S. Muller, D. Bagnard, J. P. Briand and J. Courty, *Cancer Res.*, 2011, **71**, 3296-3305.
11. B. Sulzer and A. S. Perelson, *Math Biosci*, 1996, **135**, 147-185.